Electronic structure of superlattices and quantum wells under uniaxial stress

G. Platero*
Max-Planck-Institut für Festkörperforschung Hochfeld-Magnetlabor, 166X, F-38042 Grenoble, France

M. Altarelli
Max-Planck-Institut für Festkörperforschung Hochfeld-Magnetlabor, 166X, F-38042 Grenoble, France and European Synchrotron Radiation Facility, Boîte Postale No. 220, F-38043 Grenoble Cedex, France

(Received 10 April 1987)

The envelope-function approximation is used to describe the electronic structure of superlattices and quantum wells under stress. The strain effects on the electronic properties of GaAs-$Al_xGa_{1-x}As$ quantum wells due to external in-plane stress are analyzed and compared with recent Raman and photoluminescence excitation experiments. The modification of the band structure of an InAs-GaSb superlattice due to lattice mismatch is also analyzed by means of a self-consistent calculation.

I. INTRODUCTION

Interest in the electronic structure of superlattices and quantum wells under uniaxial stresses has increased recently for several reasons. First, the development in the growth of artificial superstructures[1] allows high quality superlattices to be obtained from lattice-mismatched materials. Since the superlattice layers are thin, the lattice mismatch is accommodated by internal biaxial tensions,[2,3] which can be regarded, apart from a hydrostatic component, as uniaxial. These strained-layer superlattices provide new freedom in the choice of the layer materials, so that the number of potential superstructures increases. Moreover, the accommodation of the mismatch by elastic strains induces changes in the electronic properties qualitatively and quantitatively comparable to those due to the quantum size effects. On the other hand, uniaxial stress, which tunes the spacings between subbands, can be applied externally as a tool for analysis of the electronic states.

We perform calculations of electronic states under arbitrary unaxial stress, within the framework of the envelope-function approximation.[4–6] A six-band $\mathbf{k}\cdot\mathbf{p}$ description of the bulk band structure is adopted, neglecting the split-off valence band. The valence-band Luttinger Hamiltonian[7] is modified according to the Pikus-Bir strain Hamiltonian description,[8] already applied to heterostructures:[9]

$$H = H_{\text{Luttinger-Kohn}} + H_{\text{strain}} , \tag{1}$$

$$H_{\text{strain}} = -a(e_{xx}+e_{yy}+e_{zz}) - b[(J_x^2 - J^2/3)e_{xx} + \text{c.p.}] - \frac{2}{\sqrt{3}} d[(J_x, J_y)e_{xy} + \text{c.p.}] , \tag{2}$$

where a is the hydrostatic deformation potential, b and d the shear deformation potentials, and e_{ij} the strain tensor. The strain effects in the $\mathbf{kp}$ coupling elements between conduction and valence bands are also taken into account, following Aspnes and Cardona.[10]

The energy gap of the two materials which form the superlattice changes as a function of stress in a known way. The band offset change, however, is a poorly known quantity. In the case of internal strain in an InAs-GaSb superlattice, the experimentally determined offset[11] (which implicitly includes this effect) is used in the calculation. In the analysis of a GaAs-$Al_xGa_{1-x}As$ quantum well under external stress, however, some assumption has to be made. We follow very recent indications[12–14] that the valence-band offset in this system is essentially unchanged with pressure. Any other reasonable choice would not affect our results very much, in the 0–3-kbar range of pressure.

II. GaAs-AlGaAs QUANTUM WELLS UNDER EXTERNAL STRESS

External stress can be used to obtain information on electronic states in heterostructures. This is especially interesting for valence subbands, because of their coupled character.[15] In the absence of strain or spin-orbit interaction, the valence-band edge of diamond and zinc-blende semiconductors is a sixfold degenerate p-like multiplet. The spin-orbit interaction splits the sixfold degeneracy into a fourfold $P_{3/2}$ and a twofold $P_{1/2}$ multiplet. The application of uniaxial stress splits the $J=\frac{3}{2}$ multiplet into a pair of degenerate (nearly degenerate for the zinc-blende materials, which have no inversion symmetry) Kramers doublets, as described in Ref. 16. For example, for compressive stress along a cubic direction, the light- and heavy-hole states are split, with the light holes going up in energy. In a quantum well, with a $\langle 001 \rangle$ growth direction, the valence-band top is also split, in the absence of strain, and the heavy holes are higher in energy. If uniaxial stress is applied to the system, it

adds to the effect of confinement. If the stress direction coincides with the growth axis, the subband character remains purely heavy or light at the zone center, within the simple envelope-function scheme adopted here. For this case we recover the results obtained, by similar methods, in Ref. 9. The case of in-plane stress is more interesting. In this case the shear components mix light and heavy character of the holes at all wave vectors, including the center of the zone.

We analyze recent Raman scattering experiments on a 9-nm quantum well of GaAs-$Al_xGa_{1-x}As$, with $x=0.48$, p-doped with Be, under uniaxial (110) stress.[17] This experiment shows a strong dependence of the transitions between the different hole subbands with stress. In this case, the strain tensor is not diagonal:

$$\begin{aligned} e_{xx} &= e_{yy} = (S_{11}+S_{12})T/2 \ , \\ e_{zz} &= S_{12}T \ , \\ e_{xy} &= S_{44}T/2 \ , \\ e_{xy} &= e_{yz} = 0 \ , \end{aligned} \tag{3}$$

where S_{ij} are the compliance constants and T the stress. The Luttinger parameters, compliance constants, and deformation potentials for this system are given in Table I.

We have considered, following recent experimental information,[18] a valence-band offset equal to 40% of the band-gap difference in our calculations. The dispersion of the valence subbands was computed as a function of wave vector in the (001) plane for several values of a uniaxial (110) stress.

Figure 1(a) shows the valence subbands for the quantum well without stress. The nonparabolicity of the bands, the positive electronlike effective mass of the first light-hole subband, and the strong interaction between the different subbands are remarkable features of the diagram.

These features are reflected in the experiment, which shows different line shapes for the vertical transitions h_0-l_0 and h_0-h_1. The latter appears as a relatively narrow peak because the two subbands are nearly parallel in the region of in-plane wave vector $\mathbf{k}_\parallel$ between 0 and $\mathbf{k}_F$,

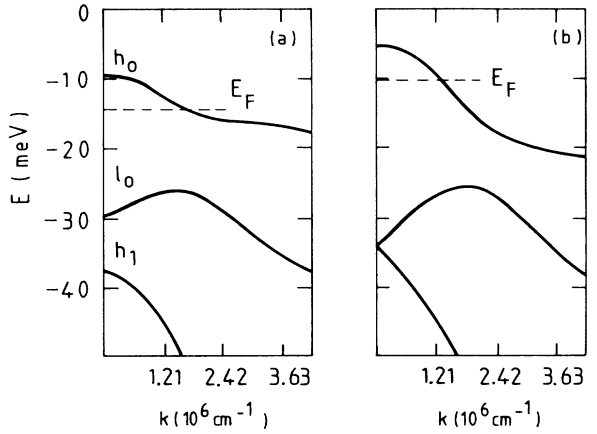

FIG. 1. Valence subband dispersion for $\mathbf{k}$ (in units of 10^6 cm^{-1}), parallel to the $\langle 110 \rangle$ stress direction of a 9-nm GaAs-$Al_{0.48}Ga_{0.52}As$ quantum well with 3×10^{11} holes per cm^2 for (a) $T=0$ and (b) $T=2.6$ kbar, where T is the stress. Energies are in meV.

while the first one gives a broad peak corresponding to the different shape for the two subbands in this $\mathbf{k}$-space region.

As we consider the external (110) uniaxial tension in our calculation, we obtain a mixing of the bands character even in the zone center. The ground heavylike subband goes up in energy while the first light and second heavylike subbands go closer to each other and nearly touch at the zone center for a pressure $T=2.6$ kbar, as is shown in Fig. 1(b). This is the behavior observed in the experiments[17] which show the broadening of the h_0-l_0 transition and its merging with the h_0-h_1 peak, and its higher energy threshold, although they take place at lower stress values than expected from the calculation. This discrepancy can be due to the input parameters of our calculation: bulk deformation potentials and band offsets, as well as the experimental uncertainty in the calibration of the stress.

TABLE I. Luttinger parameters, compliance constants, and deformation potentials for GaAs, AlAs, InAs, and GaSb. In the calculation, the compliance constants and deformation potentials for $Al_xGa_{1-x}As$ are assumed to be the same as for GaAs, while the Luttinger parameters are interpolated from their values for GaAs and AlAs.

		GaAs	AlAs	InAs	GaSb
Luttinger parameters	γ_1	6.85	3.45	3.7	3.7
	γ_2	2.1	0.68	0.6	0.6
	γ_3	2.9	1.29	0.6	0.6
Compliance constants(10^{-2} cm^2/dyn)	S_{11}	1.15		1.945	1.582
	S_{12}	−0.35		−0.685	−0.495
	S_{44}	1.657			
Deformation potentials (eV)	a	−6.7		−6.0	−8.3
	b	−1.7		−1.8	−2.0
	d	−4.55			

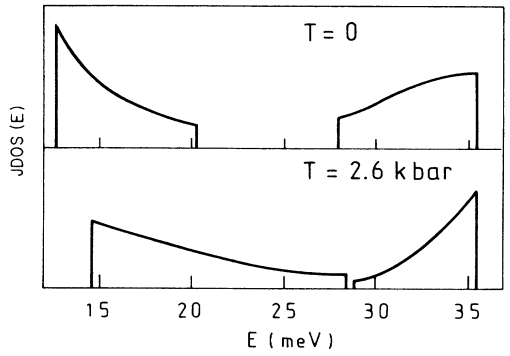

FIG. 2. Joint density of states (arbitrary units) for transitions h_0-l_0, h_0-h_1, derived from the subband structure of Fig. 1. (a) $T=0$, (b) $T=2.6$ kbar.

In Fig. 2, the joint density of states for the h_0-l_1 and h_0-h_1 transitions computed in the axial approximation is shown for $T=0$ and $T=2.6$ kbar, and the behavior described above is depicted.

Recently, photoluminescence experiments[19] were performed to investigate the uniaxial stress dependences of excitons in a GaAs-$Al_{0.3}Ga_{0.7}As$ quantum well and the effect of the quantum-well size on these dependences. We have computed the electronic structure for this quantum well under an in-plane (100) stress in the range 0–5.2 kbar.

In Fig. 3 we represent the calculated uniaxial stress dependences of the higher excitonic transitions with respect to E_{11h} (first conduction, first heavy-hole transition) in comparison with experiment. Our results agree quite well with experiments, the differences arising probably from the fact that we do not take the binding energy of the exciton, or its dependence on strain, into account.

We observe a different behavior of heavylike and lightlike holes with stress, the latter having a stronger dependence on strain. Also, a strong interaction of the transition E_{13H} and E_{11L}, as well as of E_{14H} with E_{12L} and of E_{24H} with E_{22L}, is observed.

The experimental results displayed in Fig. 3 show that one of the peaks splits into two for sufficiently large stress. This double peak was observed also in other experiments[20] and it could be due to the increase in oscillator strength of the $2p$ exciton of the E_{12H} intersubband transition, which for larger stresses acquires an intensity comparable to the $1s$ state.

Figure 4 shows the uniaxial stress dependences of E_{11H} and E_{11L} transitions with respect to their values at zero stress, as a function of well width. Three quantum wells with different well widths (22, 11 and 4 nm, respectively) are analyzed. Dashed lines represent the stress dependences of E_{11H} and E_{11L} excitons for bulk GaAs. From our calculations we obtain a different slope for these transitions, as expected, because the hydrostatic and shear components add for the E_{11L} transition (that corresponds to $J_x=\pm\frac{3}{2}$) and compensate for the E_{11H} ($J_x=\pm\frac{1}{2}$) one. One can see that the wider the well, the closer to the bulk is the behavior for both transitions. When the well is thinner, the mixed character of the subbands increases and the slopes of E_{11L} and E_{11H} are closer to each other. We obtain a qualitatively good agreement with the experiment, but smaller slopes in all cases.

III. STRAINED InAs-GaSb SUPERLATTICE

The InAs-GaSb superlattice is an interesting system because of the relative position of the band gaps of both

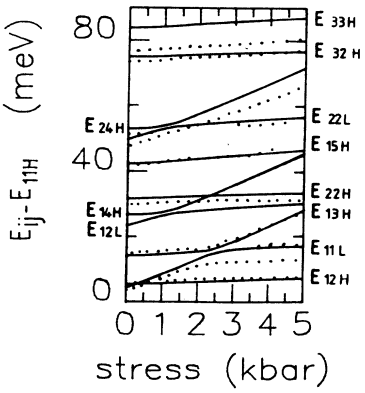

FIG. 3. The uniaxial stress dependences of higher energy excitonic transitions with respect to E_{11H}. The continuous lines represent the theoretical calculation.

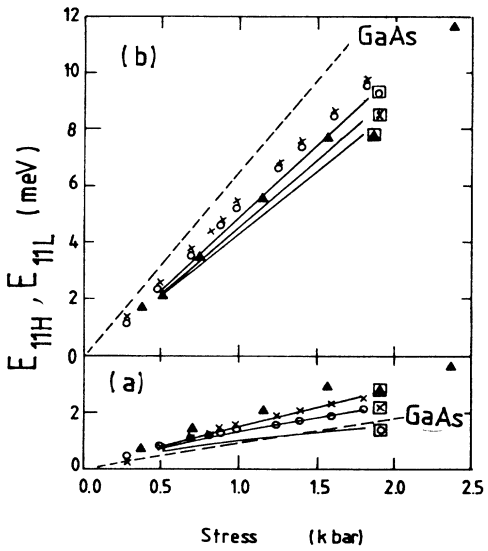

FIG. 4. The uniaxial stress dependences of (a) E_{11H} and (b) E_{11L} transitions (with respect to their $T=0$ values) as a function of well width. ▲, ×, and ○ represent a 4-nm, 11-nm, and 22-nm quantum well, respectively. The theoretical result is represented by the continuous lines. Dashed lines represent the GaAs bulk dependences for these transitions.

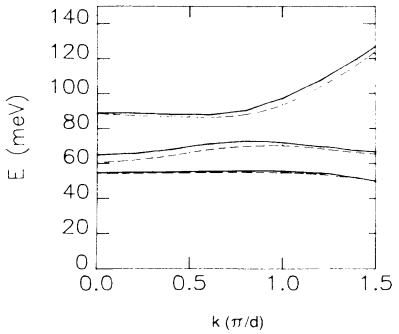

FIG. 5. Band structure of a (120,80) InAs-GaSb superlattice in the self-consistent Hartree approximation. Continuous lines represent the unstrained case and dashed lines the InAs strained case. The **k** vector is in plane and is qiven in units of π/d, where d is the superlattice period.

semiconductors: the InAs conduction-band minimum is lower in energy than the GaSb valence-band maximum and it is known that this system presents a semiconductor-semimetal transition as a function of the superlattice period.[21–24]

The difference in the lattice parameters of InAs and GaSb gives a mismatch of 0.62% with $a_{\mathrm{InAs}} < a_{\mathrm{GaSb}}$. We have included in the calculation the effects of internal strain due to the mismatch.

The nonzero components of the strain tensor in the layers of material i are[24]

$$e_{xx} = e_{yy} = \frac{(a_{\parallel} - a_i)}{a_i} = (S_{11} + S_{12}) T_i \ , \qquad e_{zz} = \frac{(a_z - a_i)}{a_i} = -2C_{12} \frac{(a_{\parallel} - a_i)}{a_i} = 2S_{12} T_i \ , \tag{4}$$

where $a_{\parallel}$ is the in-plane lattice constant and a_z the lattice constant parallel to the growth direction. The critical quantity in this system is the energy difference between the GaSb valence-band top and the InAs conduction-band minimum. The accepted value[11] for this offset is 0.15 eV and, as we do not know its dependence on strain, we therefore assume this value for the unstrained as well as for the strained case.

As the sample we consider is grown on a GaSb substrate, the lattice parameter $a_{\parallel} \approx a_{\mathrm{GaSb}}$, in this case the InAs component, is under biaxial dilation and the GaSb remains unstrained.

In Fig. 5, a self-consistent calculation is shown for the case: (a) with no tension and (b) with strain in InAs. The magnitude of this strain is of the order of 5 kbar and it produces a 46-meV splitting of light- and heavy-hole subbands plus a hydrostatic shrinkage of the fundamental gap. As a result, the conduction band is separated by 0.35 eV from the light-hole band (to be compared with the 0.41-eV gap at zero pressure), with a considerable reduction of the conduction effective mass. The effects due to strain are small, even in the case in which the GaSb is also strained (biaxial compression). This is partly an artifact of our choice to compare calculations performed with the same 0.15-eV band offset. It would be very interesting to measure the band offset in a superlattice grown on an InAs substrate. Indeed, Raman experiments[25,26] show that the choice of the substrate mainly determines the lattice parameter, so that in this case $a_{\parallel} \approx a_{\mathrm{InAs}}$, and the internal stress is different with respect to the former case. Therefore, from this experiment the band offset dependence on stress could be deduced.

IV. CONCLUSIONS

We have analyzed the effects of uniaxial strain on the electronic structure of quantum wells and superlattices, by means of the envelope-function approximation. This approximation provides a good description of the strained system, as can be seen from the comparison with Raman and photoluminescence experiments. In the latter case, it would be necessary to introduce the excitonic binding energy in the calculations and its dependence on strain in order to improve the agreement with experiment further.

ACKNOWLEDGMENTS

Numerical calculations were performed with support of the Centre de Calcul Vectoriel pour la Recherche (Palaiseau, France). One of us (G.P.) acknowledges financial support from the North Atlantic Treaty Organization (NATO).

*Permanent address: Departamento de Física del Estado Sólido, Universidad Autónoma de Madrid, Cantoblanco, 28049 Madrid 34, Spain.

[1]K. Ploog, *Crystals Growth, Properties and Applications* (Springer-Verlag, Berlin, 1980), Vol. 3, p. 73.
[2]G. C. Osbourn, J. Appl. Phys. **53**, 1586 (1982).
[3]J. W. Matthews and A. E. Blakeslee, J. Cryst. Growth **27**, 118 (1974).
[4]J. White and L. J. Sham, Phys. Rev. Lett. **47**, 879 (1981).
[5]G. Bastard, Phys. Rev. B **24**, 5693 (1981).
[6]M. Altarelli, Phys. Rev. B **28**, 842 (1983).
[7]J. M. Luttinger, Phys. Rev. **102**, 1030 (1956).
[8]G. L. Bir and G. E. Pikus, *Symmetry and Strain-Induced Effects in Semiconductors* (Wiley, New York, 1974).
[9]G. D. Sanders and Y. Chang, Phys. Rev. B **32**, 4282 (1985).
[10]D. E. Aspnes and M. Cardona, Phys. Rev. B **17**, 726 (1978).
[11]L. L. Chang, in *Semiconductor Superlattices and Heterojunctions,* edited by G. Allan, G. Bastard, N. Boccara, M. Lannoo, and M. Voss (Springer-Verlag, Berlin, 1986).
[12]D. Wolford, in *Physics of Semiconductors,* edited by O. Engstrom (World Scientific, Singapore, 1987), p. 1115.
[13]C. G. van de Walle and R. M. Martin, in *Physics of Semiconductors,* Ref. 12, p. 159.
[14]M. Cardona and N. E. Christensen, Phys. Rev. B **35**, 6182

(1987).
[15]M. Altarelli, U. Ekenberg, and A. Fasolino, Phys. Rev. B **32**, 5138 (1985).
[16]F. Pollak, *Physics of Semiconductors,* edited by S. P. Keller, J. C. Hensel, and F. Stein (United States Atomic Energy Commission, Springfield, VA 1970), p. 407.
[17]A. Pinczuk, D. Heiman, R. Sooryakumar, A. C. Gossard, and W. Wiegmann, Surf. Sci. **170**, 573 (1986).
[18]R. C. Miller, D. A. Kleinman, and A. C. Gossard, Phys. Rev. B **29**, 7085 (1984).
[19]E. S. Koteles, C. Jagannath, J. Lee, Y. J. Chen, B. S. Elmand, and J. Y. Chi, in *Physics of Semiconductors,* Ref. 12, p. 625; C. Jagannath, E. S. Koteles, J. Lee, Y. L. Chen, B. S. Elmand, and J. Y. Chi, Phys. Rev. B **34**, 7027 (1986).
[20]R. T. Collins, L. Vina, W. I. Wang, L. L. Chang, L. Esaki, K. V. Klitzing, and K. Ploog, in *Physics of Semiconductors,* Ref. 12, p. 521.
[21]L. L. Chang, J. Phys. Soc. Jpn. **49**, 997 (1980).
[22]Y. Guldner, J. P. Vieren, P. Voisin, M. Voos, L. L. Chang, and L. Esaki, Phys. Rev. Lett. **45**, 1719 (1980).
[23]J. C. Maan, Y. Guldner, J. P. Vieren, P. Voisin, M. Voos, L. L. Chang, and L. Esaki, Solid State Commun. **39**, 683 (1981).
[24]L. L. Chang, N. J. Kawai, G. A. Sai-Halasz, R. Ludeke, and L. Esaki, Appl. Phys. Lett. **35**, 939 (1979).
[25]B. Jusserand, P. Voisin, M. Voos, L. L. Chang, E. E. Mendez, and L. Esaki, Appl. Phys. Lett. **46**, 678 (1985).
[26]J. M. Calleja, F. Meseguer, C. Tejedor, E. E. Mendez, C. A. Chang, and L. Esaki, Surf. Sci. **168**, 558 (1986).